Science of the Total Environment 822 (2022) 153418

Contents lists available at ScienceDirect

Science of the Total Environment

journal homepage: www.elsevier.com/locate/scitotenv

Characterization factors and other air quality impact metrics: Case study for $PM_{2.5}$-emitting area sources from biofuel feedstock supply

Maninder P.S. Thind [a,b], Garvin Heath [a,*], Yimin Zhang [a], Arpit Bhatt [a]

[a] National Renewable Energy Laboratory, Golden, CO 80401, United States
[b] Department of Civil and Environmental Engineering, University of Washington, Seattle, WA 98195, United States

HIGHLIGHTS

- Framework and metrics for air quality planning process and LCIA
- Metrics demonstrated to a life cycle stage of biofuel production
- Application of a high-resolution, spatially-explicit air quality model – InMAP
- First area-source $PM_{2.5}$ characterization factors

GRAPHICAL ABSTRACT

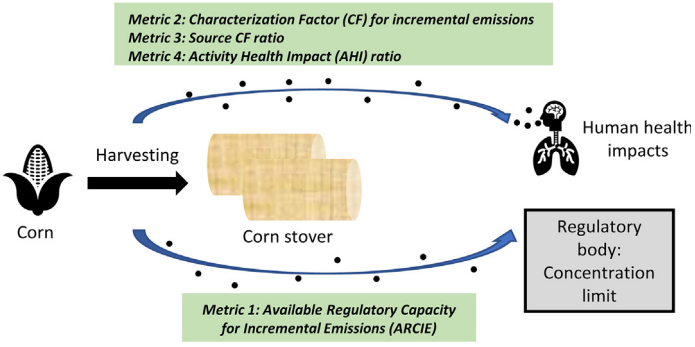

ARTICLE INFO

Article history:
Received 26 January 2020
Received in revised form 8 January 2022
Accepted 21 January 2022
Available online 29 January 2022

Editor: Pavlos Kassomenos

Keywords:
Air quality modeling
Air quality planning
Fine particulate matter
$PM_{2.5}$ health impacts
Characterization factors
Life cycle impact assessment (LCIA)
Biomass production

ABSTRACT

In this paper, we develop a framework and metrics for estimating the impact of emission sources on regulatory compliance and human health for applications in air quality planning and life cycle impact assessment (LCIA). Our framework is based on a pollutant's characterization factor (CF) and three new metrics: Available Regulatory Capacity for Incremental Emissions (ARCIE), Source CF Ratio, and Activity Health Impact (AHI) Ratio. ARCIE can be used to assess whether a receptor location has capacity to accommodate additional source emissions while complying with regulatory limits. We present CF as a midpoint indicator of health impacts per unit mass of emitted pollutant. Source CF Ratio enables comparison of potential new-source locations based on human health impacts. The AHI Ratio estimates the health impacts of a pollutant in relation to the utilization of the source for each unit of product or service. These metrics can be applied to any pollutant, energy source sector (e.g., agriculture, electricity), source type (point, line, area), and spatial modeling domain (nation, state, city, region). We demonstrate these metrics through a case study of fine particulate ($PM_{2.5}$) emissions from U.S. corn stover harvesting and local processing at various scales, representing steps in the biofuel production process. We model $PM_{2.5}$ formation in the atmosphere using a novel reduced-complexity chemical transport model called the Intervention Model for Air Pollution (InMAP). Through this case study, we present the first area-source $PM_{2.5}$ CFs that address the recommendations of several LCIA studies to establish spatially explicit CFs specific to an energy source sector or type. Overall, the framework developed in this work provides multiple new ways to consider the potential impacts of air emissions through spatially differentiated metrics.

1. Introduction

The process of siting, operating, and regulating new sources of pollutant emissions (such as power plants and factories) often entails modeling local and regional air quality impacts and predicting associated human health impacts. There is also interest in assessing full life cycle environmental

* Corresponding author at: B-263, Strategic Energy Analysis Center, National Renewable Energy Laboratory, Golden, CO 80401, United States.
E-mail address: garvin.heath@nrel.gov (G. Heath).

http://dx.doi.org/10.1016/j.scitotenv.2022.153418

impacts through life cycle impact assessment (LCIA) (Chester et al., 2010; Bulle et al., 2019). Existing LCIA research efforts have used various modeling techniques (Rosenbaum et al., 2011; Hill et al., 2009; Thakrar et al., 2017; Hill et al., 2019) and metrics such as pollutant intake fractions (iFs) (Humbert et al., 2011; Fantke et al., 2017) (the proportion of mass emitted that is inhaled by the exposed populations) and characterization factors (CFs) (Fantke et al., 2019; Gronlund et al., 2015; Tang et al., 2018) (environmental/health damage per unit of mass emitted) to analyze the air quality impacts of an energy system.

Assessing air quality and human health impacts for new emission sources often requires addressing questions from different stakeholders, such as air quality planners, project developers, and researchers. Stakeholders could be interested in understanding the impacts of emissions from new sources on the ability of counties and states to comply with regulatory requirements (such as National Ambient Air Quality Standards [NAAQS] for criteria pollutants), (NAAQS Table, 2018) comparing estimated impacts from the new source either to similar sources or to baseline emissions in a region, or estimating tradeoffs related to resources or products developed at the source (e.g., 1 unit mass of product). Careful selection of appropriate metrics for evaluation and comparison is important for answering each question.

Within LCIA, existing metrics for evaluating air quality impacts (e.g., iF and CF) are available at low-spatial-scale (resolution) emission and exposure settings—such as indoor, outdoor-urban, or outdoor-rural settings—collectively called "archetypal" environments (Humbert et al., 2011; Sedlbauer et al., 2007). Applying these metrics at these scales in LCIA can introduce significant uncertainty in the results owing to the inability to capture location-specific, pollutant-dispersion, and transformation effects. Therefore, these metrics for broad archetypal environments may provide an average estimate but generally are unsuitable for analyzing impacts for health damage-oriented LCIA studies of a specific source type (e.g., point vs. line vs. area source) or emitting sector (e.g., power generation vs. agriculture) (Humbert et al., 2011; Fantke et al., 2015). The existing process of LCIA can benefit from a consistent framework and metrics to model spatially explicit air quality and associated human health impacts of the life cycle emissions of a product or service.

Emissions of fine particulate matter ($PM_{2.5}$, which includes particles smaller than 2.5 μm in aerodynamic diameter) represent one critical area in need of improved LCIA approaches. Whether directly emitted from combustion or other activities (primary $PM_{2.5}$) or formed from precursors such as volatile organic compounds (VOCs), sulfur dioxide (SO_2), oxides of nitrogen (NO_x), and ammonia (NH_3) (secondary $PM_{2.5}$), $PM_{2.5}$ is the air pollutant that produces the largest monetized human health impacts in the United States (U.S.) and worldwide (Cohen et al., 2017; Health and Environmental Effects of Particulate Matter (PM), 2016). However, the air quality and health impacts of $PM_{2.5}$ are sensitive to the characteristics of the emitting source, geographic location, type of $PM_{2.5}$ precursor, meteorology, topography of the region, population density in the region, population age distribution, baseline mortality, and concentration-response functions derived from the air quality-related epidemiology research (Seinfeld and Pandis, 2006; Fann et al., 2009). For example, numerous LCIA studies have quantified CFs for $PM_{2.5}$ from distinct sets of archetypal environments at regional, national, and global scales (Gronlund et al., 2015; Tang et al., 2018; Hofstetter, 1998; Krewitt et al., 2001; Van Zelm et al., 2008; Itsubo and Inaba, 2010; Kassomenos et al., 2013; Notter, 2015; Van Zelm et al., 2016; Frischknecht and Jolliet, 2016; Frischknecht, 2016; Jolliet et al., 2018). Yet these studies do not distinguish $PM_{2.5}$ CFs by ground-level source type or by emitting sector. It is necessary to distinguish $PM_{2.5}$ CFs by source type (or emitting sector) to reduce uncertainty in the estimates that can arise from neglecting factors (e.g., physics and chemistry of particle formation, meteorology, characteristics of source and source location) responsible for the formation of $PM_{2.5}$ in the atmosphere and its exposure among the population. LCIA studies often do not incorporate impacts from long-range transport of $PM_{2.5}$ precursor emissions owing to the high computational requirements of computer modeling of particle formation in the atmosphere. The 2016 expert synthesis produced by the United Nations Environment Programme (UNEP) – Society of Environmental Toxicology and Chemistry's (SETAC) Life Cycle Initiative provides global consensus $PM_{2.5}$ CFs for several archetypal environments and emission stack heights (Frischknecht and Jolliet, 2016). However, the UNEP-SETAC report does not provide CFs for exposure to $PM_{2.5}$ formed from VOC emissions and does not distinguish CFs by source-type or emitting sector.

Our study makes multiple contributions to existing knowledge about characterizing air quality and health impacts in LCIA of any emission source at any location. First, we develop a framework using CF and three new metrics for estimating the impact of emissions sources on regulatory compliance and human health (defined in Section 2). These metrics provide important, new, source-specific information to quantify spatially explicit life cycle impacts. Project developers and researchers could use this new information to improve their analysis of the impacts of proposed emissions sources, which could inform decisions such as facility siting, design, and operation.

Second, we apply our new framework to a case study estimating the impacts of area-source $PM_{2.5}$ emissions from developing corn stover for cellulosic biofuel production in the U.S. This work helps respond to Fantke et al. (2015) and UNEP-SETAC (Frischknecht and Jolliet, 2016) who recommended systematically analyzing the spatial variation in secondary $PM_{2.5}$ formation rates using spatially explicit models, like the Intervention Model for Air Pollution (InMAP), (Tessum et al., 2017) and recommended estimating $PM_{2.5}$ CFs at different geographic levels (e.g., region, county). Through our case study, we develop the first estimates of area-source $PM_{2.5}$ CFs as well as the first sector-specific $PM_{2.5}$ CF estimates for the U.S. Our framework also estimates site-specific impacts on NAAQS compliance and health—relative to both national average impacts and resource production—for corn stover development. Future analyses based on these methods could provide additional resolution on air quality and health impacts by source type, sector, and location.

2. Air quality and health impacts analysis framework

Our air quality and health impacts framework is based on CF and three new metrics: Available Regulatory Capacity for Incremental Emissions (ARCIE), Source CF Ratio, and Activity Health Impact (AHI) Ratio. Fig. 1 illustrates the framework and metrics developed in this work. This framework can be applied to any source type (point, line, area) or emissions-producing sector to provide information for air quality planning and LCIA efforts. In this section, we describe the metrics in generic terms. In Section 3, we provide the specific metrics used in our case study.

2.1. Available regulatory capacity for incremental emissions (ARCIE)

ARCIE quantifies the difference between the pollutant concentration allowed by regulations and the pollutant concentration at a receptor location. It can be used to assess whether a receptor location has capacity to accommodate additional source emissions relative to the applicable regulatory limit. It is calculated as follows for a generic pollutant (PX):

$$\mathrm{ARCIE} = [\mathrm{PX}]_{\mathrm{regulated}} - [\mathrm{PX}]_{\mathrm{receptor}} \quad (1)$$

where $[PX]_{regulated}$ is the concentration of the pollutant allowed under applicable regulations, $[PX]_{receptor} = [PX]_{baseline} + [PX]_{incremental}$, $[PX]_{baseline}$ is the baseline concentration at the receptor location (prior to additional emissions from the new source), and $[PX]_{incremental}$ is the incremental concentration of additional emissions from the new source.

Thus, ARCIE indicates the effects on the regulatory cap of adding the new-source emissions. A positive value means there will still be room under the regulatory cap after the new-source emissions are added, whereas a negative value means the regulations will be exceeded after the new-source emissions are added. A zero or a negative value indicates no capacity to host additional sources that emit the pollutant. If the baseline concentration already exceeds the regulatory cap at a receptor location,

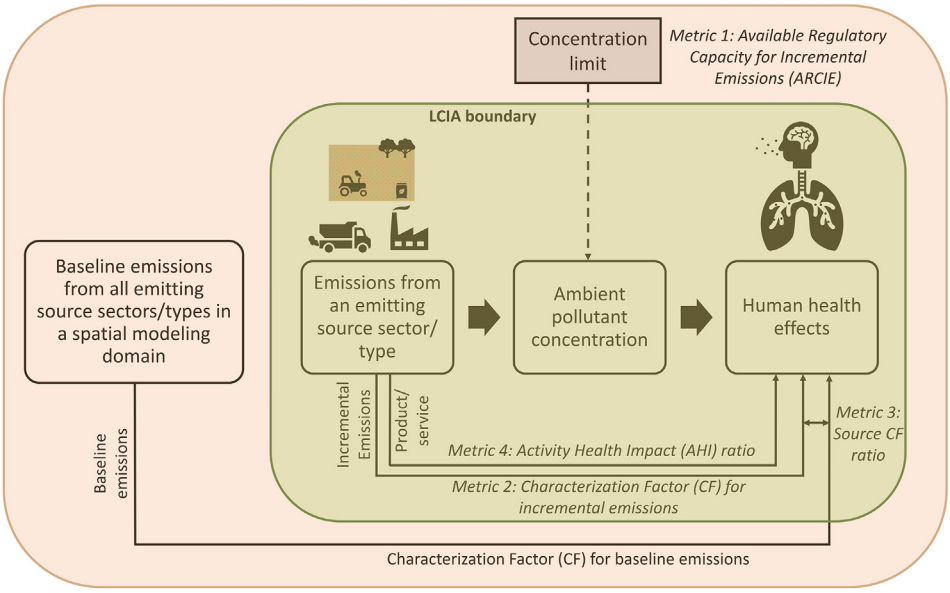

Fig. 1. Framework and metrics developed in this work for use in air quality planning and LCIA. The LCIA boundary is defined by the life cycle analysis (LCA) of an emitting source sector or type (e.g., biofuel production). The spatial modeling domain is a geographic area of which the emitting source sector or type is part and is considered for air quality modeling (e.g., country, state). Incremental emissions are additional emissions from changes in activities at the source. Metric 1 relates the concentration limit of a pollutant to the actual ambient pollutant concentration (shown separately by dashed line as it is not part of LCIA framework), metric 2 indicates impacts on the human population per unit mass of a pollutant emitted at the source, metric 3 is the ratio of CF for incremental emissions and CF for baseline emissions, and metric 4 indicates impacts on the human population per unit mass of product or service at the source.

there is zero capacity before any new-source emissions are added (and added emissions would make the ARCIE value more negative).

2.2. Characterization factor (CF)

CFs are commonly applied in the LCIA phase of LCA to quantify the health impacts caused by emissions. CFs can be reported at the midpoint or endpoint levels. A midpoint CF indicates the direct impacts of the contributing pollutants emitted at the source, including health impacts per unit of pollutant mass emitted (Van Zelm et al., 2016; Hauschild et al., 2013). An endpoint CF indicates the severity of damage modeled by the midpoint indicator, including years of life lost (YLL), years lost due to disability (YLD), and combined YLL and YLD expressed as disability-adjusted life years (DALYs) (Frischknecht and Jolliet, 2016; Hauschild et al., 2013). For this work, we focus on midpoint CF, defined as health impacts (here, premature mortality) per unit mass of primary $PM_{2.5}$ and precursor pollutant emitted and calculated using Eq. (2) (Frischknecht and Jolliet, 2016). In LCIA of an energy system, CFs can be used to estimate total impacts in a life cycle stage by multiplying the CF by the total mass of pollutant emitted.

$$\mathrm{CF} = \frac{\text{Premature mortality}}{\text{Mass of pollutant emitted}} \tag{2}$$

Premature mortality is estimated using outdoor concentration-health effect response model explained in further sections.

2.3. Source CF ratio

Source CF Ratio quantifies the incremental CF for new-source emissions in comparison to the CF for baseline emissions from all sectors in a spatial modeling domain (e.g., nation, region). It enables comparison of potential new-source locations based on human health impacts and thus can aid in ranking desirable locations. It is calculated for each pollutant as follows:

$$\text{Source CF Ratio} = \frac{\mathrm{CF}_{(\text{incremental, pollutant, new}-\text{source location})}}{\mathrm{CF}_{(\text{baseline, pollutant, spatial modeling domain})}} \tag{3}$$

where $\mathrm{CF}_{(\text{incremental, pollutant, new-source location})}$ is the CF from additional emissions of each pollutant precursor at the new-source location, and $\mathrm{CF}_{(\text{baseline, pollutant, spatial modeling domain})}$ is the CF from baseline emissions of each precursor from all pollutant-emitting sources in the spatial modeling domain. Source CF Ratio can only be used for comparison between multiple new-source locations if the spatial modeling domain in the denominator is constant across sources. A Source CF Ratio greater than one indicates that the new-source emissions have greater impacts relative to the spatial modeling domain's average impacts from baseline emissions. A Source CF Ratio less than one indicates the opposite.

2.4. Activity health impact (AHI) ratio

The AHI Ratio estimates the health impacts of a pollutant in relation to the utilization of the source, calculated as follows:

$$\text{AHI Ratio} = \frac{\text{Health impact of pollutant}}{\text{Unit of product/service}} \tag{4}$$

This metric enables quantification of the health impacts of a pollutant for each unit of product or service. For example, our case study (defined in Section 3) presents an AHI Ratio of premature deaths due to $PM_{2.5}$ per kilogram of corn stover produced.

3. Case study data and methods: impacts of $PM_{2.5}$ emissions from U.S. corn stover production

In this case study, we apply our framework from Section 2 to analyze the impacts of $PM_{2.5}$ emissions due to harvesting corn stover as a biofuel feedstock in the U.S. Corn stover—including the leaves, stalks, cobs, and husks typically left in the field (for other uses such as animal grazing and soil replenishment) after the ears of corn plants are harvested—is the most abundant source of lignocellulosic biomass in the U.S. for biofuel production (Aden et al., 2002; U.S. Department of Energy, 2016). Corn stover is collected, stored, preprocessed, and transported from agricultural fields to biofuel-producing facilities (commonly known as “biorefineries”),

consuming energy and materials during each process (Atchison and Hettenhaus, 2004).

Harvesting corn stover for biofuels also results in increased emissions of primary $PM_{2.5}$ and its precursors, (Tessum et al., 2012) which affect human health compared to the current practice (i.e., leaving corn stover in the field). Several studies have analyzed the impacts of $PM_{2.5}$ emissions related to the life cycle production and use of second-generation biofuels (biofuels derived from non-food feedstocks) (Hill et al., 2009; Thakrar et al., 2017; Cook et al., 2011; Tessum et al., 2014; Ögmundarson et al., 2020). For example, Hill et al. (2009) estimate that the U.S. $PM_{2.5}$-related health costs of cellulosic ethanol production are lower when using corn stover, switchgrass, or miscanthus as feedstocks, compared with producing gasoline or producing ethanol from corn using natural gas, coal, or corn stover for process heat at biorefineries (Hill et al., 2009). Tessum et al. (2014) model life cycle air quality impacts in the U.S. Midwest due to vehicles powered by cellulosic ethanol produced from corn stover (Tessum et al., 2014). Thakrar et al. (2017) show that the life cycle $PM_{2.5}$ health impacts from potential switchgrass production in the U.S. are dominated by NH_3 emissions from fertilizer application (Thakrar et al., 2017).

The following sections describe the data and methods we use to analyze the impacts of $PM_{2.5}$ emissions from harvesting corn stover for biofuels production in the U.S. We only consider direct emissions from corn stover harvesting and local processing, including emissions from fuel used by equipment (e.g., agricultural machinery, transport vehicles) for harvesting corn stover, fertilizer applications to compensate for lost soil nutrients, and fugitive dust emissions from machinery operations. We do not include upstream emissions, such as those related to field preparation for corn production or producing agricultural chemicals or vehicle fuels; transportation emissions due to delivering corn stover from fields to the depot or storage facilities; and emissions from converting corn stover to biofuels in a biorefinery. Fig. 2 shows various supply-chain stages in the biofuel production life cycle. In the diagram, emissions from harvesting and locally processing corn stover (highlighted in green) are considered in this study.

3.1. Corn stover data

We use corn stover production and air pollutant emissions in select U.S. counties based on the National Renewable Energy Laboratory's (NREL's) Feedstock Production Emissions to Air Model (FPEAM) and a base case from the BT16 Volume 2 study (2016 Billion-Ton Report Vol 2, 2018; Efroymson et al., 2017). We do not include biorefinery emissions in this work (Fig. 2). Key assumptions of the base case include an simulation year of 2040, 1% annual crop yield improvement, and a farmgate corn stover price of $66 per dry metric ton (DMT; dry means 0% moisture content) (Rosenbaum et al., 2011). Fig. 3 shows simulated annual county-level corn stover production in 2040 estimated by the BT16 study. To protect soil health, not all corn stover is available for bioenergy production; the fraction available depends on the U.S. Department of Agriculture (USDA) tolerable soil loss limit, wind and water erosion, maintenance of soil organic carbon, and soil nutrient recycling. These factors vary by county, resulting in 0.2%–69% of corn stover produced being available for bioenergy, with a mean of 37%. Fig. S1 in the supplement information (SI) provides county-level spatial variation in percentages of total harvested corn stover available for bioenergy. Additional details are available in the BT16 study (Efroymson et al., 2017).

3.2. Scales of corn stover production and emissions estimation at each scale

We analyze the case study at three scales of corn stover production equivalent to the amounts of feedstock required by three sizes of biorefineries in terms of DMT (1 MT = 1000 kg) of corn stover per day. We assume the stover will be used to produce infrastructure-compatible hydrocarbon fuels via a biorefinery process, which is designed to convert 2000 DMT/day of stover into 85,734 gal of renewable diesel blendstock (RDB) per day (32.9 million gasoline gallon equivalents [GGE]/year) (Davis et al., 2013). Because this throughput is very small compared to the throughput of petroleum refineries in the U.S., and it may be inadequate to meet future biofuel production requirements, we analyze two larger corn stover production scales, which can supply feedstock to two biorefinery sizes corresponding to the 5th and 10th percentiles of U.S. petroleum refinery sizes. We estimate petroleum refining capacities at these two percentiles based on the U.S. Energy Information Administration (EIA) refinery capacity database, (Refinery Capacity Report, 2018) and we calculate the required amount of corn stover for the two biorefinery sizes that can produce RDB volumes equivalent to the product throughputs (gasoline and diesel combined in terms of GGE/yr) from the two petroleum refinery capacities. The resulting three biorefinery sizes are 2000, 5200, and 9100 DMT/day.

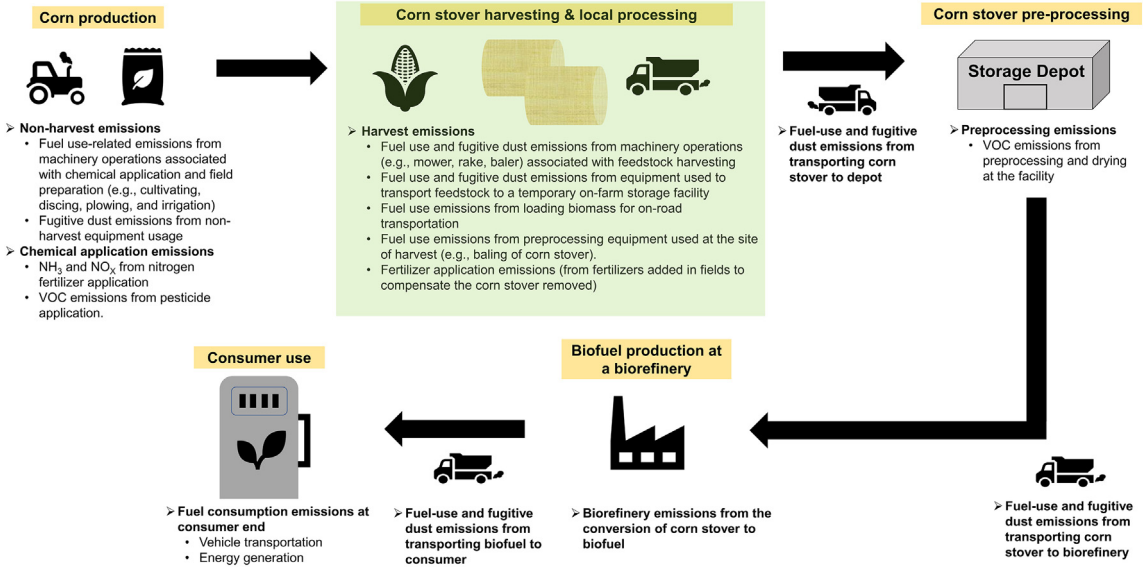

Fig. 2. Life cycle of biofuel production showing supply-chain stages and emissions from each stage. Emissions from harvesting and locally processing corn stover are considered in this study (highlighted in green). The emissions terminology used here follows the description of per-phase air emissions from the U.S. Department of Energy's 2016 Billion-Ton (BT16) Volume 2 study (GEOS-Chem Model, 2018).

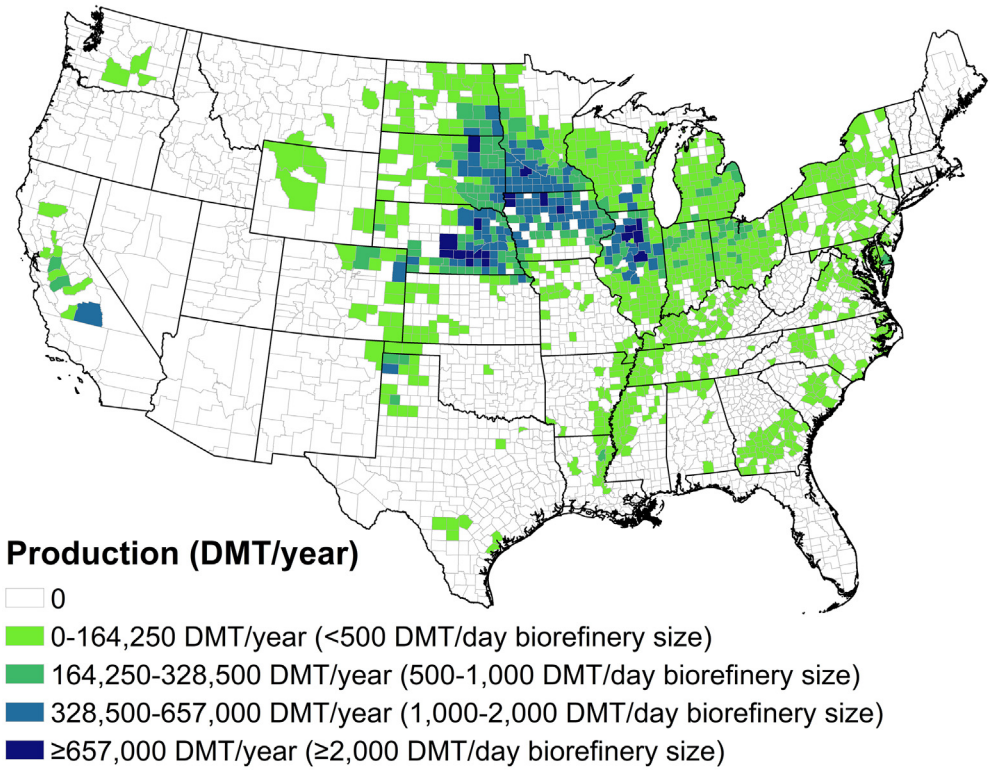

Fig. 3. Annual U.S. county-level corn stover production in 2040 from the Billion Ton 2016 base case, (GEOS-Chem Model, 2018) which assumes 1% annual crop yield improvement and a farmgate corn stover price of $66/dry metric ton (DMT). In parentheses are the biorefinery sizes for the equivalent corn stover production, calculated using Eq. (5).

We estimate the annual corn stover requirements at 657,000, 1,708,200, and 2,989,350 DMT/year (Eq. (5)).

$$\begin{aligned}\text{Corn stover required (DMT/year)} = {} & \text{biorefinery size (DMT/day)} \\ & \times 365 \text{ days/year} \\ & \times \text{on}-\text{stream operating factor}\end{aligned} \quad (5)$$

where on-stream operating factor is the percentage of time a biorefinery is operational during a year for converting biomass feedstock to biofuels; we use a factor of 90% (7884 h/year) from Davis et al. (2013). Fig. 3 shows the corn stover production for each county in the U.S. for the scenario described in Section 3.1.

Emissions at each scale of corn stover production are estimated by linear interpolation and extrapolation of BT16 emissions at the given production levels. BT16 emissions are multiplied by the ratio of corn stover production at the required scale to the production corresponding to the BT16 emissions. Details of emissions estimation at the three scales of corn stover production are provided in Section 1.2 of the SI.

3.3. County selection

From all counties in the contiguous U.S., we select 59 unique "origin" counties, defined as counties with hypothetical biorefineries located at their centroids (Fig. 4). Based on the county-level, theoretical potential supply of corn stover estimated in the BT16 study, (Efroymson et al., 2017) we identify 20 origin counties that can supply corn stover at a 2000 DMT/day scale, which we refer to as "self-sufficient" counties. No individual counties are self-sufficient to supply at a 5200 DMT/day or a 9100 DMT/day scale. From the 20 self-sufficient counties, we select eight (outlined in violet in Fig. 4) to represent the geographic diversity across the full set of 20. We assess these eight counties at all three corn stover production scales, keeping location (and the associated meteorology and population) constant while varying the scale. Section 1.3 of the SI details our county-selection methods and provides a summary table of all selected counties (Table S1).

3.4. Air quality modeling

Many air quality models are used in regulatory and research communities, each with strengths and weaknesses. Complex chemical transport models (CTMs) represent state-of-the-science models and provide the most robust estimates available when time and computational constraints are not limiting (Photochemical Air Quality Modeling, 2017; CMAQ, 2018; Comprehensive Air Quality Model with Extensions (CAMx), 2016; GEOS-Chem Model, 2018; WRF-CHEM, 2018). However, because complex CTMs are time and resource intensive, modelers can use reduced-complexity air quality models (RCMs) instead. RCMs can take a CTM-based, (Tessum et al., 2017; Buonocore et al., 2014; Carnevale et al., 2009; GEOS-Chem Adjoint Model et al., 2014; DDM/RSM Model et al., 2014; Hakami et al., 2007; EASIUR Model et al., 2016; Technical Support Document for the Proposed PM NAAQS Rule, 2006; Particle Source Apportionment Tool (PSAT) et al., 2008; Zhang et al., 2012) gaussian, (Cimorelli et al., 2005; Guttikunda, 2009; Logue et al., 2011; APEEP Model and Muller, 2014; User's Manual for the Co-Benefits Risk Assessment Health Impacts Screening and Mapping Tool (COBRA), 2012; Revision to the Guideline on Air Quality Models, 2015) lagrangian, (Draxler and Hess, 1997; Scire et al., 2000) or chemical mass balance (CMB8.2 Users Manual, 2004) approach. Although less accurate than complex CTMs, RCMs have the flexibility to allow for a greater number of sensitivity analyses, Monte Carlo approaches, an understanding of source and receptor effects, use of smaller-sized grid cells, and longer simulated periods (Hill et al., 2019; Levy et al., 2007; Keeler et al., 2016; Gourevitch et al., 2018; Millstein et al., 2017; Holland et al., 2016). Three commonly used RCMs provide comprehensive estimates covering the contiguous U.S. at relatively high spatial resolution (county level or finer): the Air Pollution Emission

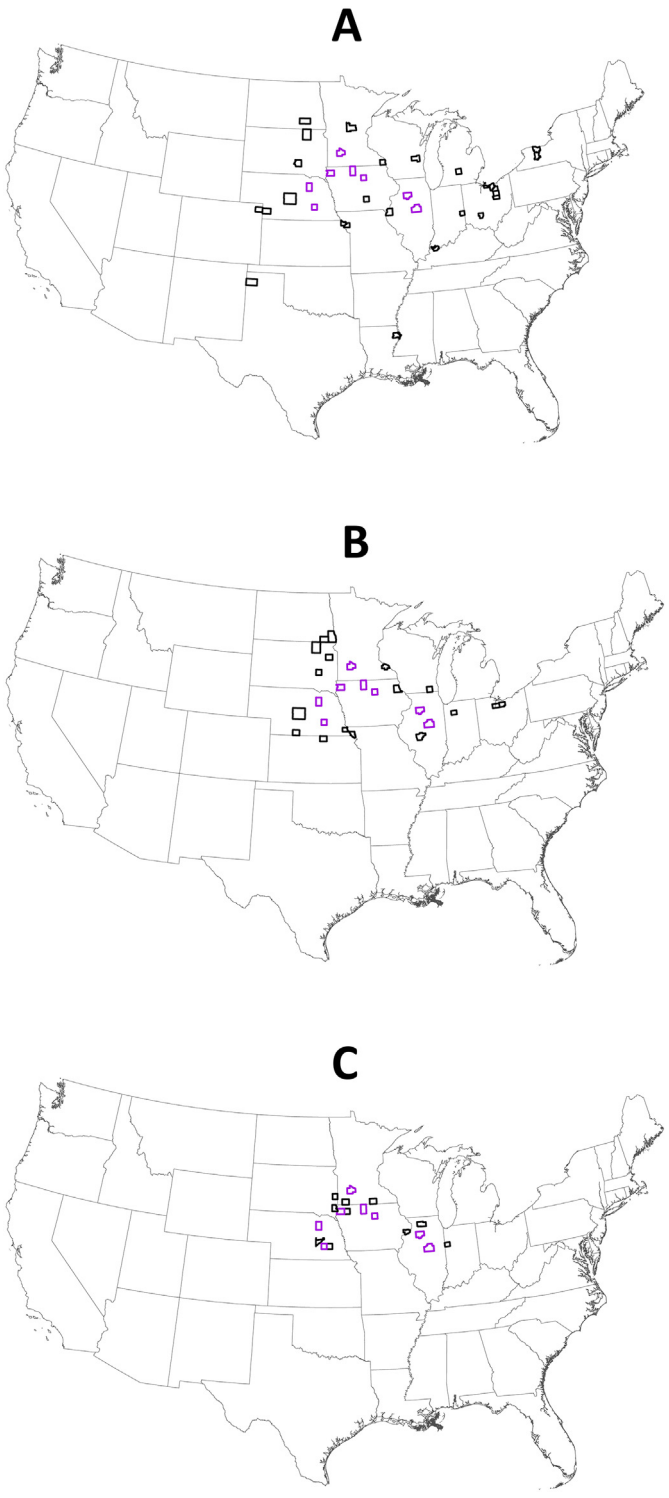

Fig. 4. Origin counties selected for air quality modeling. (A) Origin counties selected for hosting 2000 DMT/day corn stover production scale (n = 34), (B) origin counties selected for hosting 5200 DMT/day corn stover production scale (n = 25), and (C) origin counties selected for hosting 9100 DMT/day corn stover production scale (n = 18). Counties outlined in violet are "self-sufficient" counties (see text for further explanation) analyzed at all three scales of corn stover production (n = 8). Rest of the origin counties (outlined in black, that are not "self-sufficient") are surrounded by a cluster of neighboring counties (not shown in these maps) that contribute to the total requirement of the respective corn stover production scale in the origin county used in the calculations in the analysis described below (n = 51).

Experiments and Policy (APEEP/AP2) model, (APEEP Model and Muller, 2014) the Estimating Air pollution Social Impacts Using Regression (EASIUR) model, (EASIUR Model et al., 2016) and InMAP (Tessum et al., 2017). Gilmore et al. (2019) compare these three models. Among the three, APEEP/AP2 has county-level spatial resolution, EASIUR uses a 36 km × 36 km grid covering the contiguous U.S., and InMAP employs smaller-sized grid cells at much finer-scale spatial resolution than any other RCMs. While APEEP/AP2 can model concentrations from all $PM_{2.5}$ precursors, EASIUR cannot model formation of secondary organic aerosols (SOA) from VOC emissions; hence, EASIUR cannot currently be used to estimate total $PM_{2.5}$. APEEP/AP2 has lower spatial resolution (county-level) than InMAP does, which is not desirable for estimating metrics developed in this work.

Therefore, we use InMAP for our analysis. InMAP is designed to estimate the annual average $PM_{2.5}$ concentration and health impacts resulting from incremental changes in pollutant emissions (Tessum et al., 2017). It estimates average pollutant concentrations from emissions by estimating a steady-state solution to a mass-balance equation dependent on reaction, advection, and diffusion parameters. Geographic locations in InMAP can be specified as polygon, line, or point sources (including stack-height and plume-rise attributes, where relevant). InMAP uses a variable spatial grid, where the grid cell size is a function of the gradient in population density and pollutant concentrations, varying from 1 km × 1 km (typically, in urban areas) to 48 km × 48 km (typically, in rural areas). As described below, InMAP uses a Concentration-Response (C-R) function to estimate health impacts from the resulting pollutant concentration. The output from InMAP provides pollutant concentration ($\mu g/m^3$) and number of premature deaths from long-term $PM_{2.5}$ exposure for each grid cell based on underlying gridded population and mortality data.

The following are the three main inputs to InMAP for our case study:

(1) County-level annual emissions of VOCs, NO_x, NH_3, SO_2, and primary $PM_{2.5}$ for selected counties. Separate area-source Geographic Information System (GIS) shapefiles are created for a county or group of counties producing corn stover at three scales, and InMAP is run for each county or group of counties separately. InMAP allocates emissions from area (county) shapefiles to the underlying grid cells using area weighting.
(2) Census data on population at the block group level for 2013 from the 2013 American Community Survey (ACS, 5-year data between 2009 and 2013) (The IPUMS National Historical Geographic Information System (NHGIS), 2018).
(3) Baseline all-cause mortality data at the county level for 2013 from the National Center for Health Statistics Office of Analysis and Epidemiology at the Centers for Disease Control and Prevention (CDC Wonder, 2018).

Consistent with prior research (Buonocore et al., 2014; GEOS-Chem Adjoint Model et al., 2014; Fann et al., 2013; Penn et al., 2017; Levy et al., 2009) and in keeping with United States Environmental Protection Agency (US EPA) norms, (U.S. EPA, 2019; Expanded Expert Judgment Assessment of the Concentration-Response Relationship Between PM2.5 Exposure and Mortality (Final Report), n.d.; Health Benefits of the Second Section 812 Prospective Study of the Clean Air Act, 2010) we assume that all particles are equally toxic in estimating health impacts from total $PM_{2.5}$. InMAP is capable of estimating health impacts from any user-defined C-R function. For this work, we employ the standard, commonly used expression in InMAP—from Krewski et al. (2009)—for our $PM_{2.5}$C-R function, which is used to estimate $PM_{2.5}$-related health impacts as shown in Eq. (6). The Krewski et al. (2009) equation is based on the standard Cox proportional-hazards model to calculate hazard ratios for various cause-of-death categories associated with the levels of air pollution exposure in the study cohort. The default C-R equation in InMAP is a standard and is commonly used in regulatory (U.S. EPA, 2019) and academic air quality research in the U.S. (Thakrar et al., 2017; Hill et al., 2019) Premature death is defined

as a death that would have occurred later in a population in the absence of $PM_{2.5}$ pollution (Schwartz et al., 2018).

$$\text{No.of premature deaths} = \left(e^{(\text{PM2.5 Linear Coefficient} \times [\text{PM2.5}])} - 1\right) \times P \times \frac{\text{All} - \text{Cause Mortality Rate}}{100,000} \quad (6)$$

where $PM_{2.5}$ Linear Coefficient = ln (1.078)/10 = 0.00751, i.e., a 7.8% increase in the number of premature deaths for every 10 μg/m^3 increase in the concentration of $PM_{2.5}$. $[PM_{2.5}]$ is the concentration of $PM_{2.5}$. P is total population.

3.5. Case study metrics

We express the results of our analysis in terms of the metrics defined in Section 2, for each selected origin county and corn stover production scale; see Section 2 for general definitions of the variables used in the equations below. We define the case-specific ARCIE for the selected origin counties of corn stover production as follows. For this metric, we chose EPA's outdoor air quality monitor locations—used for measuring $PM_{2.5}$ concentrations and designating areas as attainment, maintenance, or non-attainment (Air Quality Designations for Particle Pollution, 2018) —as our receptor locations.

$$\text{ARCIE} = [PM_{2.5}]_{NAAQS} - [PM_{2.5}]_{receptor} \quad (7)$$

where $[PM_{2.5}]_{NAAQS}$ is the annual ambient $PM_{2.5}$ concentration limit under EPA's 2012 NAAQS, 12.0 μg/m^3 (annual mean, averaged over 3 years), as a primary standard for providing public health protection, (NAAQS Table, 2018) $[PM_{2.5}]_{receptor} = [PM_{2.5}]_{baseline} + [PM_{2.5}]_{incremental}$, $[PM_{2.5}]_{baseline}$ is the annual average baseline $PM_{2.5}$ concentration at the monitor locations (background annual average $PM_{2.5}$ concentration, prior to additional emissions from the corn stover production), and $[PM_{2.5}]_{incremental}$ is the annual average incremental $PM_{2.5}$ concentration of additional emissions from the corn stover production at the monitor location. We use 2017 data (most recent available at the time of the analysis) for annual average $PM_{2.5}$ concentration (from real-time measured values) at each monitor as $[PM_{2.5}]_{baseline}$ (Air Data, 2018). Thus, $[PM_{2.5}]_{receptor}$ is the total annual average $PM_{2.5}$ concentration at the monitor locations accounting for baseline emissions from all emissions source sectors, plus the incremental concentration from the new source—corn stover production.

As per EPA rules, (40 CFR Parts 50, 2013) the annual $PM_{2.5}$ NAAQS is met when the "annual $PM_{2.5}$ NAAQS design value (DV)" is less than or equal to 12.0 μg/m^3 at each eligible monitoring site. The "annual $PM_{2.5}$ NAAQS DV" is the 3-year average of $PM_{2.5}$ annual average mass concentrations for each eligible monitoring site (40 CFR Parts 50, 2013). The DV is rounded to the nearest tenth of a μg/m^3, that is, the actual highest value possible that is below the standard is 12.04 μg/m^3. Intermediate calculations for estimating DVs are not rounded as per EPA rules (40 CFR Parts 50, 2013). In this work, we make two assumptions for comparing with the NAAQS limit of 12.0 μg/m^3 ($[PM_{2.5}]_{NAAQS}$): (1) at each monitor location, we use a 1-year annual average $PM_{2.5}$ concentration ($[PM_{2.5}]_{baseline}$, $[PM_{2.5}]_{incremental}$), not the 3-year average, and (2) we do not use any rounding convention for the 1-year annual average $[PM_{2.5}]_{receptor}$, assuming this estimation is analogous to an intermediate step in EPA's procedure for estimating DV. In addition, EPA's relative response factor (RRF) approach to reduce uncertainty of concentration estimates has not been considered for the InMAP modeled concentration here (Modeling Guidance for Demonstrating Air Quality Goals for Ozone, 2018). With these simplifying assumptions, the ARCIE metric cannot be used as a true indicator of available capacity for the selected corn stover production cases. Rather, it serves as an initial, screening-level indicator to identify sites that might face challenges complying with $PM_{2.5}$ NAAQS owing to new emissions and may require additional analysis.

Counties are deemed capable of hosting additional corn stover production if ARCIE is greater than zero for all EPA air quality monitors. For monitors that are already in EPA NAAs, (2012 Annual PM2.5 Designations, 2018) any increase in modeled incremental concentration would lead to additional challenges in meeting the NAAQS.

We define the case-specific CF for the origin counties of corn stover production via Eq. (8), using the midpoint CF of premature deaths per kg $PM_{2.5}$ precursor emitted:

$$\text{CF}_{\text{source,precursor}} = \frac{\text{Premature deaths}}{\text{Mass of } PM_{2.5} \text{ precursor (kg)}} \quad (8)$$

We report CF for each selected origin county discussed in Section 3.3 (Fig. 4), at the national scale and for each downwind U.S. county. For each downwind county, we compute total premature deaths from each $PM_{2.5}$ precursor by aggregating premature deaths in each InMAP grid cell to the county scale. Similarly, to report CF at the national scale, we aggregate premature deaths in each grid cell to the national scale. Mass of $PM_{2.5}$ precursor (kg) in the denominator is estimated by aggregating emissions from each source county supplying corn stover at each scale.

We define the case-specific Source CF Ratio for the origin counties of corn stover production as follows, where the CF in the denominator relates to all $PM_{2.5}$ precursor source emissions at the national level (contiguous U.S.):

$$\text{Source CF Ratio} = \frac{\text{CF}_{(\text{incremental,precursor,location})}}{\text{CF}_{(\text{baseline,precursor,national})}} \quad (9)$$

We estimate the Source CF Ratio for each $PM_{2.5}$ precursor separately. The baseline emissions for estimating the denominator of $CF_{baseline,\ precursor,\ national}$ are from 2014 EPA National Emissions Inventory (NEI) data (2014 National Emissions Inventory (NEI) Data, 2019). We aggregate emissions from each $PM_{2.5}$-emitting source in the contiguous U.S. for estimating total baseline emissions. We calculate total premature deaths from each $PM_{2.5}$ precursor at national scale by aggregating deaths in each InMAP grid cell across the U.S. $CF_{(incremental,\ precursor,\ location)}$ for each origin county location is estimated similarly to $CF_{source,\ precursor}$ at the national scale (Eq. (8)).

Finally, we define the case-specific AHI Ratio for each origin county as follows:

$$\text{AHI Ratio} = \frac{\text{Premature deaths from total } PM_{2.5}}{\text{Corn stover production (kg)}} \quad (10)$$

Premature deaths from total $PM_{2.5}$ are estimated by aggregating deaths from total $PM_{2.5}$ (all precursors) in each InMAP grid cell to the national scale. Corn stover production (kg) is estimated using Eq. (5) (multiplied by the factor of 1000 kg/DMT) at each corn stover production scale.

4. Case study: results and discussion

We provide results in terms of the four metrics defined in our analytical framework: ARCIE, CF, Source CF Ratio, and AHI Ratio. The results presented in our case study are based on a subset of counties to demonstrate our methods and metrics identified—they should not be taken as conclusive. The metrics are useful at the screening level to inform decisions about areas that are suitable or unsuitable for siting new emissions sources.

4.1. ARCIE: impact of corn stover production on regulatory compliance

We estimate ARCIE for locations downwind of all the origin counties across the three corn stover production scales. We develop maps for spatially visualizing the regulatory impact at EPA monitor locations. An example origin county in Illinois (IL), McLean county (Federal Information Processing Standard [FIPS] county code: 17113, self-sufficient at a corn stover production scale of 2000 DMT/day) was selected for illustrative purposes because it is analyzed at all three scales of corn stover production. Fig. 5 shows example results for the McLean county, IL, for each corn stover

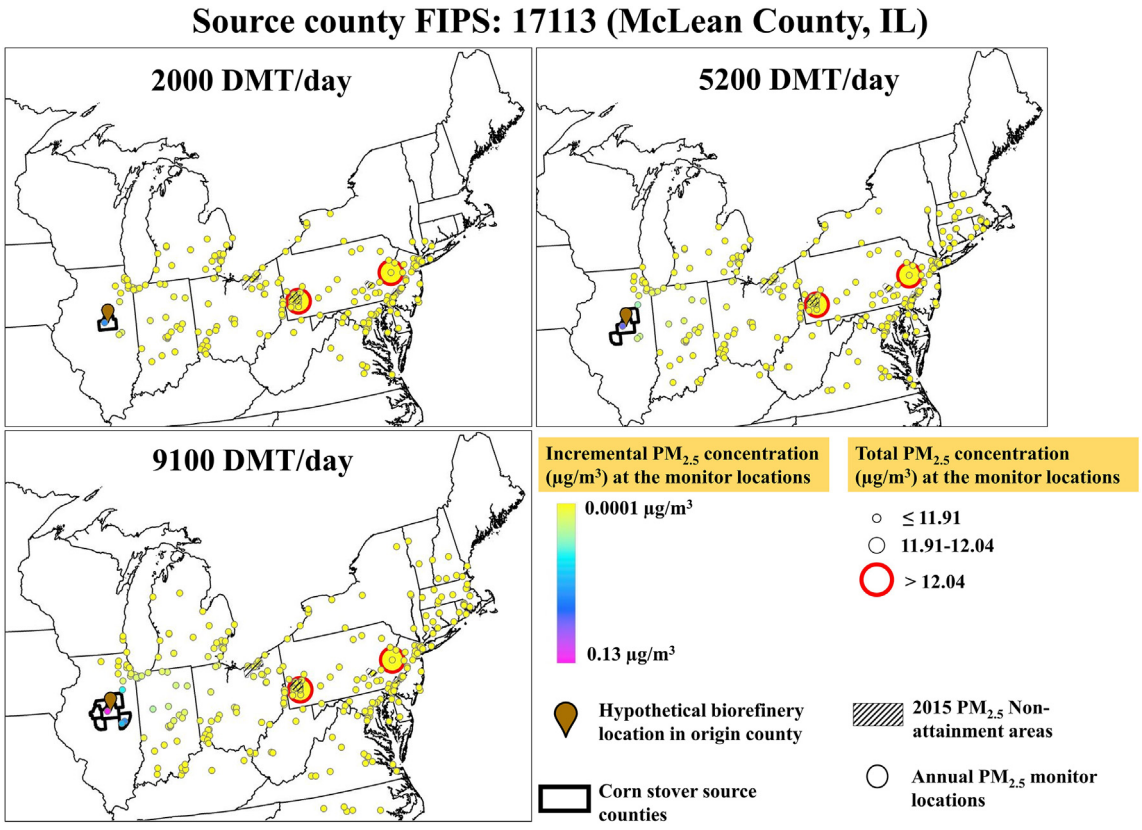

Fig. 5. Example of Available Regulatory Capacity for Incremental Emissions (ARCIE) results depicting total $PM_{2.5}$ concentration (μg/m^3) and incremental $PM_{2.5}$ concentration (μg/m^3) from harvesting and local processing emissions from an example origin county (FIPS 17113: McClean County, Illinois) at three corn stover production scales. The maps show only those monitors that have incremental concentrations greater than 0.0001 μg/m^3. Variations in colors at the monitor locations show the incremental $PM_{2.5}$ concentration between 0.0001 μg/m^3 and 0.13 μg/m^3 (maximum incremental concentration for the 9100 DMT/day scale). Circle sizes show the total $PM_{2.5}$ concentration ($[PM_{2.5}]_{receptor}$) at the monitor location, which is the sum of baseline and incremental $PM_{2.5}$ concentrations. Our analysis is designed to test whether new emission sources cause changes in monitor concentrations such that a monitor concentration at baseline below the NAAQS annual average $PM_{2.5}$ concentration limit (12.04 μg/m^3) might potentially increase to above the NAAQS limit. Implementing this design in creating an ability to visualize such a circumstance, we chose ranges of total concentrations as explained here. We focus on total concentration changes around the $PM_{2.5}$ annual NAAQS of 12.0 μg/m^3 at the accuracy of one tenth of a μg/m^3 applicable in the NAAQS criteria (Burnett et al., 2018). That is, the actual highest value possible that is below the standard is 12.04 μg/m^3. The threshold value of 11.91 μg/m^3 is the difference between 12.04 μg/m^3 and the maximum incremental concentration value, 0.13 μg/m^3. This value helps in identifying any cases of "flipping" for the 9100 DMT/day scale. In this example, we find no cases of flipping in any of the corn stover production scales. All of the monitor locations show only the lowest incremental increase in $PM_{2.5}$ concentration, except those closest to the source counties. The red circles highlight monitors with total $PM_{2.5}$ concentrations (as well as the baseline concentrations) above the NAAQS limit, yet none of these locations exceeded the NAAQS limit because of the additional corn stover production.

production scale. Not surprisingly, as the scale increases, the incremental concentration increases at the nearest monitor locations. We also identify any cases of monitor "flipping"—a monitor is considered flipped if the $PM_{2.5}$ concentration at the monitor location increases to above the $PM_{2.5}$ NAAQS limit of 12.0 μg/m^3. For McLean county, no monitor location is flipped. Fig. 5 also shows the $PM_{2.5}$ NAAs (available at the time, shown with diagonal stripe pattern) for 2015 and $[PM_{2.5}]_{receptor}$ > 12.04 μg/m^3 at a monitor location (shown with red circles). $PM_{2.5}$ NAAs and monitors with $[PM_{2.5}]_{receptor}$ > 12.04 μg/m^3 may not overlap, because we use 2017 data for $PM_{2.5}$ baseline concentrations, and $PM_{2.5}$ NAAs are a function of 3-year averages of $PM_{2.5}$ annual average concentrations during 2013–2015. Not surprisingly, incremental concentrations are very low at monitors distant from the source county because the source emissions are at ground level. Thus, for this example, the impact on $PM_{2.5}$ NAAs is negligible. Results for the other origin counties are presented in SI Figs. S3, S4, and S5.

Table S2 shows example ARCIE values for all the monitors in Illinois that are impacted by corn stover production at a scale of 9100 DMT/day from the origin, McLean county. The ARCIE values range from 1.7–4.9 μg/m^3, indicating that the overall maximum capacity for additional $PM_{2.5}$ emissions is 1.7 μg/m^3, considering impact on in-state monitors only. ARCIE values for the other origin counties at each scale are also provided in the SI (as Excel files).

Fig. 6 summarizes the maximum incremental $PM_{2.5}$ concentrations and maximum ARCIE values at monitor locations within the 17 corn stover producing states across the seven USDA regions. In Fig. 6, we focus on in-state monitors for two reasons: (1) State Implementation Plans (SIPs) are developed for emission sources within the state boundaries, and (2) emissions from corn stover production are at ground-level and demonstrate negligible impact on monitors far from the source counties. Among all the corn stover production cases considered here, the most impacted in-state (and overall U.S.) monitors have incremental $PM_{2.5}$ concentrations of 0.08 μg/m^3 for 2000 DMT/day, 0.1 μg/m^3 for 5200 DMT/day, and 0.13 μg/m^3 for 9100 DMT/day. Maximum in-state ARCIE varies between 0.7 and 4.4 μg/m^3 for all cases and does not vary significantly across corn stover production scales. ARCIE is positive for all the monitors that are already below the NAAQS limit; that is, all origin counties have capacity to host new activities at the three scales of emissions tested. For monitors that have baseline concentrations greater than the NAAQS limit, incremental concentrations vary and are higher if the origin counties are nearby. A few origin counties in Ohio are near 2015 $PM_{2.5}$ NAAs in Ohio; for those origin counties, the incremental concentration at the monitors in NAAs varies from 0.03–0.04 μg/m^3. The air quality planners in the NAAs can benefit from these results when developing SIPs to ensure the plans account for the impact of distributed area emissions that are near the NAAs.

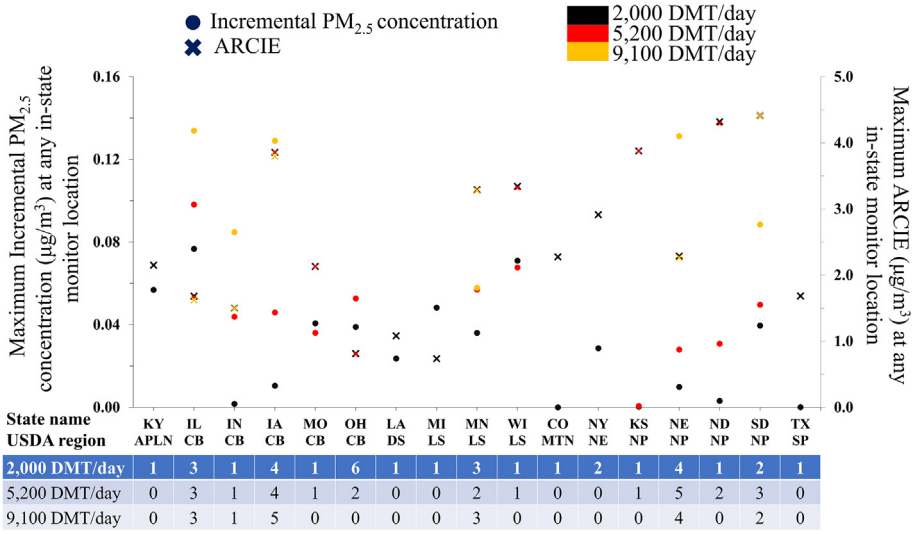

Fig. 6. Maximum in-state incremental $PM_{2.5}$ concentration (shown on left y-axis, solid circle) and maximum in-state ARCIE (shown on right y-axis, solid x) at a monitor location from all origin counties in the 17 corn stover producing states across seven USDA regions (shown on x-axis below state abbreviations). USDA regions are APLN: Appalachian, CB: Corn belt, DS: Delta states, LS: Lake states, MTN: Mountain, NE: North East, NP: Northern plains, and SP: Southern plains. Symbol colors differentiate results for each corn stover production scale. Listed below x-axis in the table are the number of origin counties in each state that are analyzed at each corn stover production scale: 2000, 5200, and 9100 DMT/day. For example, in Kentucky, only one origin county is analyzed, at the 2000 DMT/day scale.

Across all the origin counties assessed, none of the monitors at any production scale are flipped by the additional corn stover emissions. To evaluate complete impacts on the regulatory limit from the biofuel production supply chain, emissions from biorefineries (as point, elevated sources) and other parts of the supply chain (see Fig. 2) can be added to observe any flipping of the monitors. Additionally, annual $PM_{2.5}$ monitors do not cover locations in the entire U.S., so impacts at the receptor locations where monitors do not exist cannot be evaluated. As a sensitivity analysis, we use Land Use Regression (LUR) model estimates of $PM_{2.5}$ at each centroid of census blocks (at ~1 km scale) (Kim et al., 2020) as baseline concentrations and find that some receptor locations flip owing to incremental concentration from the source counties. However, if EPA's rounding convention for estimating $PM_{2.5}$ DVs is used, we observe no flipping of monitors.

Although ARCIE is useful to gain a screening-level understanding of the impacts of increased $PM_{2.5}$ emissions on the $PM_{2.5}$ regulatory limit, many factors contribute to $PM_{2.5}$ NAA designations, which limits the use of this metric in our case study. Some general factors—in addition to the air quality data of monitors that set the area boundaries—are population density, expected population growth, and degree of urbanization.

4.2. CF: health impacts per unit of $PM_{2.5}$ from corn stover production

Table 1 shows midpoint CFs by precursor type for 18 origin counties that can host a biorefinery at a scale of 9100 DMT/day corn stover production. CFs for the 2000 and 5200 DMT/day cases are shown in SI Tables S3 and S4. The CFs vary by origin county and precursor. For example, the SO_2 CF for origin county FIPS 17141 is four times higher than it is for origin county FIPS 46101. $PM_{2.5}$ CFs by precursor type for each impacted county downwind of source counties are included in the SI as GIS shapefiles. Example maps of county-scale CFs for primary $PM_{2.5}$ at the 9100 DMT/day scale are presented in SI Fig. S6.

4.3. Source CF ratio: health impacts of different corn stover production locations

Fig. 7 shows Source CF Ratios by $PM_{2.5}$ precursor type for 18 origin counties at a corn stover production scale of 9100 DMT/day. Results for

Table 1
Midpoint $PM_{2.5}$ characterization factors (CFs; in deaths per kg pollutant emitted at the source) by precursor type for all the origin counties selected at a corn stover production scale of 9100 DMT/day (results for the two other scales can be found in the SI).

Origin county FIPS	Origin county state	Primary $PM_{2.5}$	SO_2	NO_x	NH_3	VOC
17141	IL	2.2×10^{-5}	8.2×10^{-6}	3.1×10^{-6}	1.7×10^{-5}	1.0×10^{-6}
17011	IL	1.7×10^{-5}	7.4×10^{-6}	2.8×10^{-6}	1.3×10^{-5}	8.8×10^{-7}
17113	IL	9.2×10^{-6}	4.5×10^{-6}	2.5×10^{-6}	7.7×10^{-6}	7.3×10^{-7}
18007	IN	8.6×10^{-6}	4.5×10^{-6}	2.6×10^{-6}	7.5×10^{-6}	7.0×10^{-7}
19141	IA	3.5×10^{-6}	2.1×10^{-6}	1.7×10^{-6}	3.4×10^{-6}	3.8×10^{-7}
19163	IA	1.3×10^{-5}	6.3×10^{-6}	2.6×10^{-6}	1.0×10^{-5}	7.8×10^{-7}
19069	IA	5.2×10^{-6}	3.4×10^{-6}	2.0×10^{-6}	4.9×10^{-6}	4.7×10^{-7}
19109	IA	3.9×10^{-6}	2.6×10^{-6}	1.7×10^{-6}	3.8×10^{-6}	3.9×10^{-7}
19167	IA	3.6×10^{-6}	2.0×10^{-6}	1.7×10^{-6}	3.4×10^{-6}	3.9×10^{-7}
27047	MN	4.5×10^{-6}	2.2×10^{-6}	1.7×10^{-6}	3.7×10^{-6}	4.2×10^{-7}
27105	MN	3.4×10^{-6}	2.0×10^{-6}	1.6×10^{-6}	3.2×10^{-6}	3.6×10^{-7}
27127	MN	4.5×10^{-6}	2.3×10^{-6}	1.5×10^{-6}	3.5×10^{-6}	3.8×10^{-7}
31121	NE	3.9×10^{-6}	2.3×10^{-6}	1.8×10^{-6}	3.8×10^{-6}	4.6×10^{-7}
31159	NE	4.4×10^{-6}	2.6×10^{-6}	1.8×10^{-6}	4.1×10^{-6}	4.8×10^{-7}
31003	NE	2.9×10^{-6}	2.1×10^{-6}	1.6×10^{-6}	3.2×10^{-6}	3.5×10^{-7}
31185	NE	3.8×10^{-6}	2.4×10^{-6}	1.8×10^{-6}	3.8×10^{-6}	4.3×10^{-7}
46083	SD	3.9×10^{-6}	2.0×10^{-6}	1.8×10^{-6}	3.4×10^{-6}	4.2×10^{-7}
46101	SD	3.4×10^{-6}	1.9×10^{-6}	1.5×10^{-6}	3.0×10^{-6}	3.5×10^{-7}

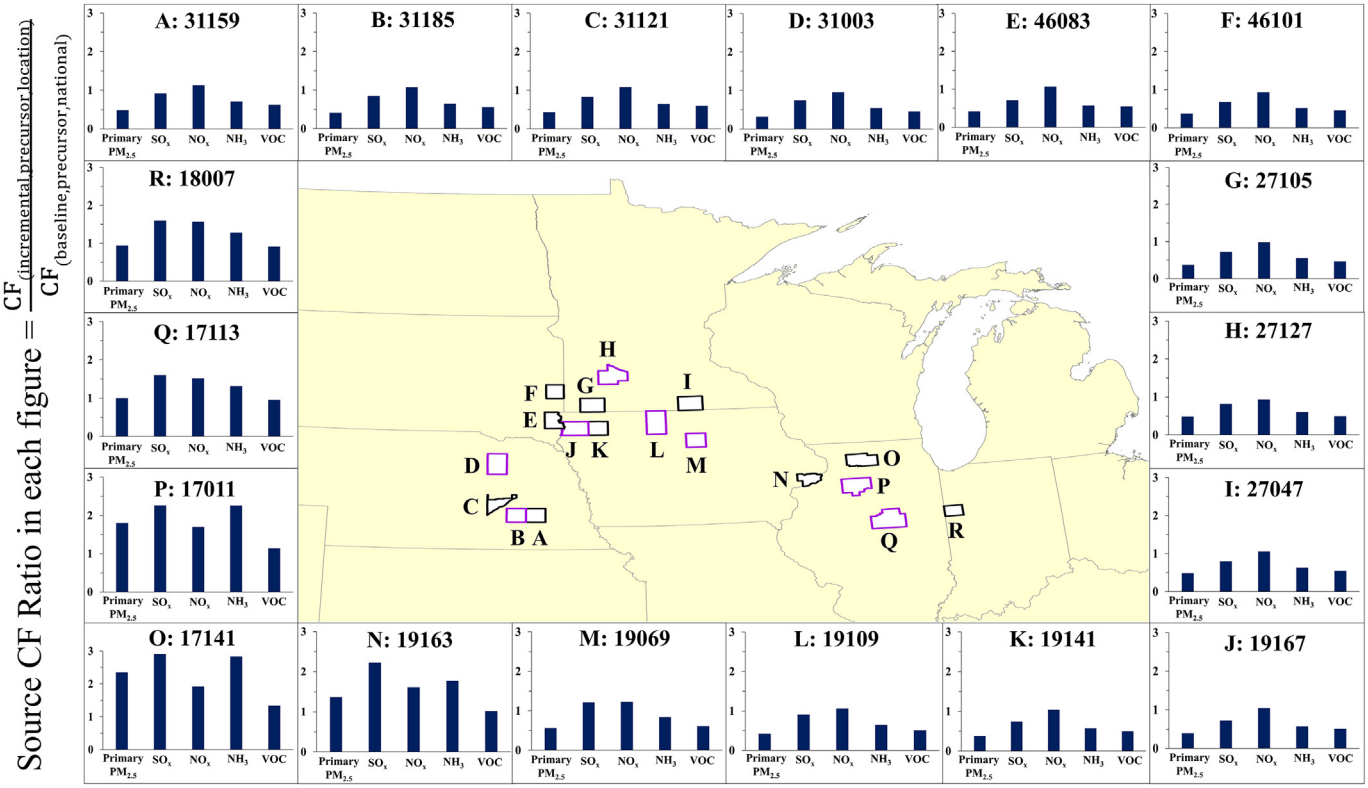

Fig. 7. Source CF ratios (y-axis of each plot) by $PM_{2.5}$ precursor type (x-axis) for all origin counties at a corn stover production scale of 9100 DMT/day. Origin counties outlined in violet are the "self-sufficient" cases at the corn stover production scale of 2000 DMT/day (see text for further explanation). The title for each plot is the county FIPS code. Figures for the other two scales can be found in SI.

the 2000 and 5200 DMT/day cases are provided in SI Figs. S7 and S8. A Source CF Ratio greater than 1 suggests that relative health impacts for the origin county are greater than the national-average impact per kg of precursor emitted. In Fig. 7, for example, the relative impacts of primary $PM_{2.5}$ are greater than national-average impacts for origin counties FIPS 19163, 17,141, and 17,011. Source CF Ratios can aid in site selection. For example, almost all origin counties in Illinois and Indiana and one in Iowa (19163) have larger relative impacts than the rest of the origin counties in Minnesota, Nebraska, South Dakota, and Iowa. Thus, origin counties in Illinois and Indiana may not be the desirable locations to site new-source emissions considering the larger relative human health impacts. If, for example, a decision-maker must site production in Illinois, then county FIPS 17113 might be the best choice owing to its lower relative impact compared to the state's other locations.

4.4. AHI ratio: health impacts per unit mass of corn stover production

Fig. 8 shows the AHI Ratio for each of the 18 origin counties at a corn stover production scale of 9100 DMT/day. Results for the other production scales are presented in SI Figs. S9 and S10. On average, cases of corn stover production in Illinois have the largest health impact per kg of production. The AHI Ratio pattern is similar to the Source CF Ratio pattern across origin counties and production scales.

4.5. Health impacts at different corn stover production scales

We analyze eight origin counties at all three corn stover production scales. As expected, CF, Source CF Ratio, and AHI Ratio generally increase with increasing scale. For example, for McLean county (origin county, FIPS 17113) in Illinois, CF and Source CF Ratio increase by 2%–8% across precursors as the scale increases (with the exception of NO_x and VOC, which demonstrate a slight decrease as the scale increases from 2000 to 5200 DMT/day); see Table 2. AHI Ratio follows the same general pattern. Metric comparisons between scales for all eight origin counties are provided in SI Tables S6 and S7.

5. Discussion and conclusions

In this work, we develop a framework based on CF and three new metrics (ARCIE, Source CF Ratio, and AHI Ratio) to characterize air quality impacts of a pollutant for use in air quality planning and LCIA of any emitting sector or source type, in any spatial modeling domain, and to aid in siting new-source emissions. We illustrate use of these metrics through a case study of $PM_{2.5}$ emissions from U.S. corn stover harvesting and local processing at various scales, representing steps in the biofuel production process. $PM_{2.5}$ formation is modeled using InMAP, a novel reduced-complexity and computationally inexpensive air quality model that offers high-spatial-resolution analysis. Using spatially explicit exposure and health effect outputs from the InMAP model, this work attempts to respond to recommendations from the UNEP-SETAC report to estimate spatially explicit $PM_{2.5}$ CFs (Frischknecht and Jolliet, 2016).

Each metric serves a different purpose. Although the simplifying assumptions underlying the ARCIE metric make it unsuitable for direct application in the regulatory context, ARCIE provides an initial indication of whether anticipated pollutant emissions from an emitting sector or source type could lead to nonattainment of regulatory concentration limits, yielding a capacity for additional emissions in terms of pollutant concentration. Future work could formulate a similar metric in terms of additional pollutant mass that can be emitted without violating regulatory limits at the receptor locations.

CF is a useful weighting factor employed in LCIA for estimating damage from various impact categories. For our case study, we report estimates of area-source $PM_{2.5}$ CFs by each precursor type. Estimated CFs vary by source county location, size, and scale. We are the first to quantify area-source CFs for an area-source sector. Our area-source CFs for corn stover harvesting can be put into context of CFs for other source types, for instance to point

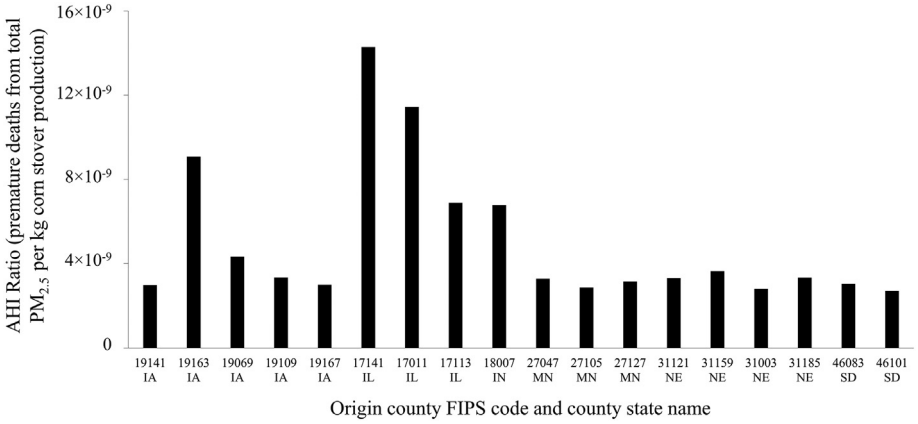

Fig. 8. Activity Health Impact (AHI) ratio for all the origin counties at a corn stover production scale of 9100 DMT/day; total $PM_{2.5}$ includes primary and secondary $PM_{2.5}$. The x-axis shows the county FIPS code and the state of the origin county. Figures for the other two scales can be found in SI.

sources hypothetically emitting either from ground level or a tall stack (such as a power plant or industrial facility). For this comparison, we retrieve CFs provided in InMAP's Source-Receptor Matrix (ISRM) (Download, 2021) for the two comparison source types assumed to be emitting from the same source counties as evaluated for corn stover production (Table S8). We find that the median of our CFs is of the same order of magnitude as those reported in the ISRM, with a small higher directional bias (higher by 8–42% and 3–68% than typical ground-level and high stack point source, respectively). This comparison indicates that harvesting corn stover at the magnitude of production scales analyzed in this work could have comparable or potentially higher health damages per unit precursor mass (CF) than a point source emitting either at ground-level or from a high stack. The comparison reflects a balance of the differences between the two source types compared (source type (point vs. area) and release height (elevated or ground-level)): point sources concentrate emissions at the release point, which can lead to higher downwind concentrations within the zone of influence whereas area sources spread emissions across large areas; ground-level emissions lead to higher ground-level concentrations than do emissions released at significant height off of the ground. Our comparison is illustrative for the counties and specific characteristics of the sources studied (e.g., a single, hypothetical stack height was chosen) and may not be more generally true for all configurations of either area or high stack point sources. Future research efforts could more systematically compare the CFs between area, line, and point source types.

Source CF Ratio aids in site selection based on the health impacts of source locations compared with national average impacts by pollutant type. AHI Ratio provides a simple factor that links human health impacts to products or services created at the source. For our case study, Source CF Ratio by precursor type and AHI Ratio vary across origin counties and scales of production—an expected result, because $PM_{2.5}$ health impacts depend on many factors including emission source strength, location and emitting source characteristics, wind speed, meteorology, and population density. Future work could explore the sensitivity of these metrics to changes in source strength.

In this work, we do not provide central tendency estimates for the cases tested in our case study because we haven't explored enough cases to derive representative central tendency estimates. We test only limited cases to demonstrate our methods. Additionally, the air quality model used in this work does not allow for uncertainty analysis of the model outputs.

In this work, we estimate CFs using ambient $PM_{2.5}$ concentration as the exposure metric. Prior studies have recommended the use of population intake fraction as the default exposure metric for computing $PM_{2.5}$-related health impacts in LCIA. However, our approach is appropriate for our case study which is centered in the US where the average $PM_{2.5}$ concentrations are low (typically less than 12 $\mu g/m^3$ annual average $PM_{2.5}$ concentration) and where the US EPA continues to use and recommend a linear concentration-response function (U.S. EPA, 2019). In the future, the CF cases examined here could be replicated using a full impact pathway (emissions - fate - intake - effect factors) utilizing intake fractions as a measure of the population's ambient $PM_{2.5}$ exposure and compared to the results reported here (Fantke et al., 2019). Such future, being beyond the scope of this study, could enhance understanding of the sensitivity of CFs to the choice of estimation approach.

Our selection of concentration-response (C-R) function reflects the one most commonly used in the scientific literature (Thakrar et al., 2017; Hill et al., 2019) and by the US EPA (e.g., U.S. EPA, 2019): a mortality hazard ratio of 1.078 for all-cause mortality from the American Cancer Society (ACS) re-analysis study (Krewski et al., 2009) which is a linear C-R function with no threshold. To understand the impact of alternative mortality hazard ratios on the CFs calculated in this work, a sensitivity analysis can be performed using a range of alternative values from Lepeule et al. (2012) (i.e., reanalysis of the Harvard Six Cities (H6C) study) [1.14, 95% CI = 1.07–1.22], Vodonos et al. (2018) [1.129, 95% CI = 1.109–1.150], and Pope et al. (2019) [1.12, 95% CI = 1.08–1.15]. These alternative hazard ratios increase the CFs estimated in this work by: 75% (Lepeule et al., 2012), 62% (Vodonos et al., 2018), and 51% (Pope et al., 2019). Detailed quantification of uncertainty in the C-R, via meta-analysis or other techniques, is outside the scope of research for this article, however, these comparisons

Table 2
CF, Source CF Ratio, and AHI Ratio comparisons between production scales for one example origin county, McLean county (FIPS 17113) in Illinois. Tables for the other 7 "self-sufficient" counties can be found in SI.

	CF					Source CF Ratio					AHI Ratio
	Primary $PM_{2.5}$	SO_2	NO_x	NH_3	VOC	Primary $PM_{2.5}$	SO_2	NO_x	NH_3	VOC	Total $PM_{2.5}$
2000 DMT/day	8.4×10^{-6}	4.2×10^{-6}	2.4×10^{-6}	7.2×10^{-6}	7.0×10^{-7}	0.91	1.5	1.5	1.2	0.91	6.5×10^{-9}
5200 DMT/day	8.6×10^{-6}	4.4×10^{-6}	2.4×10^{-6}	7.3×10^{-6}	6.8×10^{-7}	0.93	1.6	1.5	1.3	0.88	6.6×10^{-9}
9100 DMT/day	9.2×10^{-6}	4.5×10^{-6}	2.5×10^{-6}	7.7×10^{-6}	7.3×10^{-7}	1.00	1.6	1.5	1.3	0.95	6.9×10^{-9}
% change 2000 to 5200	2%	6%	−2%	2%	−3%	2%	6%	-2%	2%	-3%	2%
% change 5200 to 9100	7%	2%	3%	5%	8%	7%	2%	3%	5%	8%	4%

suggest that our CF results are conservative relative to other options for C-R function available in the literature, i.e., likely underestimate the true health impacts per unit pollutant emitted from the source. Future work can test the results using state-of-the-science C-R functions including functions that are non-linear in nature (Pope et al., 2015; Burnett et al., 2018). In addition, future research on $PM_{2.5}$C-R functions could explore whether C-R function might depend in part on source sector, geographical region, or chemical constituents.

In conclusion, the framework and metrics developed in this work could be applied in air quality planning process to quantify the available regulatory capacity as well as damage caused by pollutant emissions in different supply-chain stages of an LCA. The methods can guide industrial strategic planning and procedures such as siting, facility design, and facility operation. At the same time, the methods can be used to weigh tradeoffs between the benefits of development (such as increased employment or reduced greenhouse gas intensity) and the impacts (such as degraded air quality and health outcomes).

CRediT authorship contribution statement

Maninder P.S. Thind: Conceptualization, Methodology, Data curation, Software, Formal analysis, Investigation, Writing – original draft, Visualization. **Garvin Heath:** Conceptualization, Methodology, Writing – review & editing, Supervision, Project administration, Resources, Funding acquisition. **Yimin Zhang:** Conceptualization, Methodology, Writing – review & editing, Supervision. **Arpit Bhatt:** Conceptualization, Methodology, Data curation, Writing – review & editing.

Declaration of competing interest

The authors declare that they have no known competing financial interests or personal relationships that could have appeared to influence the work reported in this paper.

Acknowledgements

We greatly thank Rebecca Locker and Cynthia Randles for their support and valuable thoughts on our methods and results and for many helpful discussions. We thank Prof. Julian Marshall, Dr. Chris Tessum, Dr. Vikram Ravi, and Dr. Daniel Inman for their comments and suggestions to improve this research. We sincerely thank Jarett Zuboy for his contribution in improving the writing of the paper. This work was supported by the U.S. Department of Energy (DOE) under Contract No. DE-AC36-08GO28308 with Alliance for Sustainable Energy, LLC, the operator of the National Renewable Energy Laboratory, and ExxonMobil Research and Engineering (EMRE) under Agreement FIA-17-01861. The views expressed in the article do not necessarily represent the views of EMRE, DOE, or the U.S. Government. The U.S. Government retains and the publisher, by accepting the article for publication, acknowledges that the U.S. Government retains a nonexclusive, paid-up, irrevocable, worldwide license to publish or reproduce the published form of this work, or allow others to do so, for U.S. Government purposes.

Appendix A. Supplementary data

Supplementary data to this article can be found online at https://doi.org/10.1016/j.scitotenv.2022.153418.

References

2012 Annual PM2.5 Designations, 2018. U.S. Environmental Protection Agency: Washington, DC. https://epa.maps.arcgis.com/apps/MapJournal/index.html?appid=a76e14f777de49baa5d32f5544c8e20b&webmap=fc297672dd074e4ab5b208aebe21fa52.

2014 National Emissions Inventory (NEI) Data, 2019. U.S. Environmental Protection Agency: Washington, DC. https://www.epa.gov/air-emissions-inventories/2014-national-emissions-inventory-nei-data (accessed 5 February 2018).

2016 Billion-Ton Report Vol 2, 2018. U.S. Department of Energy: Washington, DC. https://www.bioenergykdf.net/billionton2016vol2 (accessed 22 November 2018).

Aden, A., Ruth, M., Ibsen, K., Jechura, J., Neeves, K., Sheehan, J., et al., 2002. Lignocellulosic Biomass to Ethanol Process Design and Economics Utilizing Co-current Dilute Acid Prehydrolysis and Enzymatic Hydrolysis for Corn Stover; NREL/TP-510-32438. National Renewable Energy Laboratory (NREL), Golden, CO.

Air Data, 2018. Air Quality Data Collected at Outdoor Monitors Across the US. U.S. Environmental Protection Agency, Washington, DC (assessed 29 April 2019) https://aqs.epa.gov/aqsweb/airdata/download_files.html.

Air Quality Designations for Particle Pollution, 2018. U.S. Environmental Protection Agency: Washington, DC. https://www.epa.gov/particle-pollution-designations (assessed 29 April 2019).

APEEP ModelMuller, N.Z., 2014. Boosting GDP growth by accounting for the environment. Science 345 (6199), 873–874. https://doi.org/10.1126/science.1253506.

Atchison, J.E., Hettenhaus, J.R., 2004. Innovative Methods for Corn Stover Collecting, Handling, Storing and Transporting; NREL/SR-510-33893. National Renewable Energy Laboratory (NREL), Golden, CO (accessed 27 April 2019) https://www.nrel.gov/docs/fy04osti/33893.pdf.

Bulle, C., Margni, M., Patouillard, L., Boulay, A.M., Bourgault, G., De Bruille, V., Cao, V., Hauschild, M., Henderson, A., Humbert, S., Kashef-Haghighi, S., Kounina, A., Laurent, A., Levasseur, A., Liard, G., Rosenbaum, R.K., Roy, P.O., Shaked, S., Fantke, P., Jolliet, O., 2019. IMPACT World+: a globally regionalized life cycle impact assessment method. Int. J. Life Cycle Assess. 24, 1653–1674.

Buonocore, J.J., Dong, X., Spengler, J.D., Fu, J.S., Levy, J.I., 2014. Using the community multiscale air quality (CMAQ) model to estimate public health impacts of PM2.5 from individual power plants. Environ. Int. 68, 200–208.

Burnett, R., Chen, H., Szyszkowicz, M., et al., 2018. Global estimates of mortality associated with long-term exposure to outdoor fine particulate matter. PNAS 115, 9592–9597.

Carnevale, C., Finzi, G., Pisoni, E., Volta, M., 2009. Neuro-fuzzy and neural network Systems for air Quality Control. Atmos. Env. 43, 4811–4821.

CDC Wonder, 2018. Center for Disease Control and Prevention, Atlanta, GA. https://wonder.cdc.gov/ (assessed 18 August 2018).

Chester, M., Pincetl, S., Bunje, P., Zahn, L., 2010. Life-cycle Assessment and Urban Sustainability; CEC-500-2013-129. California Energy Commission, Sacramento, CA.

Cimorelli, A.J., Perry, S.G., Venkatram, A., Weil, J.C., Paine, R.J., Wilson, R.B., Lee, R.F., Peters, W.D., Brode, R.W., 2005. AERMOD: A dispersion model for industrial source applications. Part I: general model formulation and boundary layer characterization. J. Appl. Meteorol. 44, 682–693.

CMAQ, 2018. The Community Multiscale Air Quality Modeling System; U.S. Environmental Protection Agency, Washington, DC. https://www.epa.gov/cmaq (accessed 20 February 2018).

CMB8.2 Users Manual, 2004. Tech. Rep. U.S. Environmental Protection Agency, Washington, DC. http://www3.epa.gov/ttn/scram/models/receptor/EPA-CMB82Manual.pdf.

Cohen, A.J., Brauer, M., Burnett, R., Anderson, H.R., Frostad, J., Estep, K., Balakrishnan, K., Brunekreef, B., Dandona, L., Dandona, R., Feigin, V., Freedman, G., Hubbell, B., Jobling, A., Kan, H., Knibbs, L., Liu, Y., Martin, R., Morawska, L., Pope, C.A.I.I.I., Shin, H., Straif, K., Shaddick, G., Thomas, M., van Dingenen, R., van Donkelaar, A., Vos, T., Murray, C.J.L., Forouzanfar, M.H., 2017. Estimates and 25-year trends of the global burden of disease attributable to ambient air pollution: an analysis of data from the global burden of diseases study 2015. Lancet 389, 1907–1918.

40 CFR Parts 50 52, 51., 2013. National Ambient Air Quality Standards for Particulate Matter; Final Rule. U.S. Environmental Protection Agency, Washington, DC (accessed 21 November 2018) https://www.gpo.gov/fdsys/pkg/FR-2013-01-15/pdf/2012-30946.pdf.

Comprehensive Air Quality Model with Extensions (CAMx), 2016. Environ International Corporation, Novato, CA. http://www.camx.com/home.aspx (accessed 20 February 2018).

Cook, R., Phillips, S., Houyoux, M., Dolwick, P., Mason, R., Yanca, C., Zawacki, M., Davidson, K., Michaels, H., Harvey, C., Somers, J., Luecken, D., 2011. Air quality impacts of increased use of ethanol under the United States' energy Independence and security act. Atmos. Environ. 45, 7714–7724.

Davis, R., Tao, L., Tan, E.C.D., Biddy, M.J., Beckham, G.T., Scarlata, C., et al., 2013. Process Design and Economics for the Conversion of Lignocellulosic Biomass to Hydrocarbons: Dilute-acid and Enzymatic Deconstruction of Biomass to Sugars and Biological Conversion of Sugars to Hydrocarbons; NREL/TP-5100-60223. National Renewable Energy Laboratory (NREL), Golden, CO.

DDM/RSM ModelFoley, K.M., Napelenok, S.L., Jang, C., Phillips, S., Hubbell, B.J., Fulcher, C.M., 2014. Two reduced form air quality modeling techniques for rapidly calculating pollutant mitigation potential across many sources, locations and precursor emission types. Atmos. Environ. 98, 283–289.

Download, Data, 2021. The Center for Air, Climate, and Energy Solutions. U.S. Environmental Protection Agency, Washington, DC (accessed 7 June 2021) https://www.caces.us/data.

Draxler, R.R., Hess, G.D., 1997. Description of the HYSPLIT 4 Modeling System. Tech. rep. NOAA Technical Memorandum ERL ARL-224: Silver Spring, MD. https://www.arl.noaa.gov/documents/reports/arl-224.pdf.

EASIUR ModelHeo, J., Adams, P.J., Gao, H.O., 2016. Reduced-form modeling of public health impacts of inorganic PM2.5 and precursor emissions. Atmos. Env. 137, 80–89 Tokyo (in Japanese).

U.S. Department of Energy. In: Efroymson, R.A., Langholtz, M.H., Johnson, K.E., Stokes, B.J. (Eds.), 2016 Billion-Ton Report: Advancing Domestic Resources for a Thriving Bioeconomy, Volume 2: Environmental Sustainability Effects of Select Scenarios from Volume 1; Chapter 9, ORNL/TM-2016/727; Oak Ridge National Laboratory, Oak Ridge, TN (accessed 20 March 2019) https://bioenergykdf.net/sites/default/files/BillionTonDownloads/BillionTon_Report_2016_vol2_Chapter9.pdf.

Expanded Expert Judgment Assessment of the Concentration-Response Relationship Between PM2.5 Exposure and Mortality (Final Report), .. Office of Air Quality Planning and Standards, U.S. Environmental Protection Agency, Research Triangle Park, NC, September

2006. Prepared by: Industrial Economics, Incorporated, Cambridge, MA. (assessed 18 August 2018) https://www3.epa.gov/ttnecas1/regdata/Uncertainty/pm_ee_report.pdf.
Fann, N., Fulcher, C.M., Hubbell, B.J., 2009. The influence of location, source, and emission type in estimates of the human health benefits of reducing a ton of air pollution. Air Qual. Atmos. Health 2, 169–176.
Fann, N., Fulcher, C.M., Baker, K., 2013. The recent and future health burden of air pollution apportioned across US sectors. Environ. Sci. Technol. 47, 3580–3589.
Fantke, P., Jolliet, O., Evans, J.S., Apte, J.S., Cohen, A.J., Hänninen, O.O., Hurley, F., Jantunen, M.J., Jerrett, M., Levy, J.I., Loh, M.M., Marshall, J.D., Miller, B.J., Preiss, P., Spadaro, J.V., 2015. Health effects of fine particulate matter in life cycle impact assessment: conclusions from the Basel guidance workshop. Int. J. Life Cycl. Assess. 20, 276–288.
Fantke, Peter, Jolliet, Olivier, Apte, Joshua S., Hodas, Natasha, Evans, John, Weschler, Charles J., Stylianou, Katerina S., Jantunen, Matti, McKone, Thomas E., 2017. Characterizing aggregated exposure to primary particulate matter: recommended intake fractions for indoor and outdoor sources. Environ. Sci. Technol. 51, 9089–9100.
Fantke, P., McKone, T.E., Tainio, M., Jolliet, O., Apte, J.S., Stylianou, K.S., Illner, N., Marshall, J.D., Choma, E.F., Evans, J.S., 2019. Global effect factors for exposure to fine particulate matter. Environ. Sci. Technol. 53 (12), 6855–6868.
Frischknecht, 2016. Global guidance on environmental life cycle impact assessment indicators: progress and case study. Int J Life Cycle Assess 21, 429–442.
Frischknecht, R., Jolliet, O., 2016. Global Guidance for Life Cycle Impact Assessment Indicators. Vol. 1. UNEP/SETAC Life Cycle Initiative, Paris, France.
GEOS-Chem Adjoint ModelDedoussi, I.C., Barrett, S.R.H., 2014. Air pollution and early deaths in the United States. Part II: attribution of PM2.5 exposure to emissions species, time, location and sector. Atmos. Environ. 99, 610–617.
GEOS-Chem Model, 2018. Atmospheric Chemistry Modeling Group, Harvard University, Cambridge, MA. http://acmg.seas.harvard.edu/geos/index.html (accessed 20 February 2018).
Gilmore, E.A., Heo, J., Muller, N.Z., Tessum, C.W., Hill, J., Marshall, J., Adams, P.J., 2019. An inter-comparison of air quality social cost estimates from reduced-complexity models. Environ. Res. Lett. 14, 074016.
Gourevitch, J.D., Keeler, B.L., Ricketts, T.H., 2018. Determining socially optimal rates of nitrogen fertilizer application. Agric. Ecosyst. Environ. 254, 292–299.
Gronlund, C.J., Humbert, S., Shaked, S., O'Neill, M.S., Jolliet, O., 2015. Characterizing the burden of disease of particulate matter for life cycle impact assessment. Air Qual. Atmos. Health 8, 29–46.
Guttikunda, S.K., 2009. SIM-Air Modeling Tools. UrbanEmissions.info. http://www.urbanemissions.info/tools/ (accessed 5 February 2018).
Hakami, A., Henze, D.K., Seinfeld, J.H., Singh, K., Sandu, A., Kim, S., Byun, D., Li, Q., 2007. The adjoint of CMAQ. Environ. Sci. Technol. 41, 7807–7817.
Hauschild, M.Z., Goedkoop, M., Guinée, J., Heijungs, R., Huijbregts, M., Jolliet, O., Margni, M., Schryver, A.N., Humbert, S., Laurent, A., Sala, S., Pant, R., 2013. Identifying best existing practice for characterization modeling in life cycle impact assessment. Int. J. Life Cycle Assess. 18, 683–697.
Health and Environmental Effects of Particulate Matter (PM), 2016. U.S. Environmental Protection Agency: Washington, DC. https://www.epa.gov/pm-pollution/health-and-environmental-effects-particulate-matter-pm (accessed 1 January 2019).
Health Benefits of the Second Section 812 Prospective Study of the Clean Air Act, 2010. Review of EPA's DRAFT. Science Advisory Board, U.S. Environmental Protection Agency, Washington, DC.
Hill, J., Polasky, S., Nelson, E., Tilman, D., Huo, H., Ludwig, L., Neumann, J., Zheng, H., Bonta, D., 2009. Climate change and health costs of air emissions from biofuels and gasoline. Proc. Natl. Acad. Sci. U. S. A. 106, 2077–2082.
Hill, J., Goodkind, A., Tessum, C., Thakrar, S., Tilman, D., Polasky, S., Smith, T., Hunt, N., Mullins, K., Clark, M., Marshall, J., 2019. Air-quality-related health damages of maize. Nat. Sustain. 2, 397–403.
Hofstetter, P., 1998. Perspectives in life cycle impact assessment, a structured approach to combine models of the technosphere, ecosphere and valuesphere. Kluwer Academic Publishers, Dordrecht (accessed 22 November 2018) http://www.springer.com/la/book/9780792383772.
Holland, S.P., Mansur, E.T., Muller, N.Z., Yates, A.J., 2016. Damages and expected deaths due to excess NOx emissions from 2009 to 2015 volkswagen diesel vehicles. Environ. Sci. Technol. 50, 1111–1117.
Humbert, S., Marshall, J.D., Shaked, S., Spadaro, J.V., Nishioka, Y., Preiss, P., McKone, T.E., Horvath, A., Jolliet, O., 2011. Intake fraction for particulate matter: recommendations for life cycle impact assessment. Environ. Sci. Technol. 45, 4808–4816.
Itsubo, N., Inaba, A., 2010. LIME2 life-cycle impact assessment method based on endpoint modeling. JEMAI Tokyo (in Japanese).
Jolliet, O., Antón, A., Boulay, A., Cherubini, F., Fantke, P., Levasseur, A., McKone, T.E., Michelsen, O., Motoshita, M., Pfister, S., Verones, F., Vigon, B., Frischknecht, R., Milà i Canals, L., 2018. Global guidance on environmental life cycle impact assessment indicators: impacts of climate change, fine particulate matter formation, water consumption and land use. Int. J. Life Cycl. Assess. https://doi.org/10.1007/s11367-018-1443-y.
Kassomenos, P.A., Dimitriou, K., Paschalidou, A.K., 2013. Human health damage caused by particulate matter PM10 and ozone in urban environments: the case of Athens, Greece. Environ. Monit. Assess. 185, 6933–6942.
Keeler, B.L., Gourevitch, J.D., Polasky, S., Isbell, F., Tessum, C.W., Hill, J.D., Marshall, J.D., 2016. The social costs of nitrogen. Sci. Adv. 2, e1600219.
Kim, S.Y., Bechle, M.J., Hankey, S., Sheppard, L., Szpiro, A.A., Marshall, J.D., 2020. Concentration of criteria pollutants in the contiguous U.S., 1979–2015: role of prediction model parsimony in integrated empirical geographic regression. PLoS One 15 (2), e0228535. https://doi.org/10.1371/journal.pone.0228535.
Krewitt, W., Trukenmuller, A., Bachmann, T.M., Heck, T., 2001. Country-specific damage factors for air pollutants. Int. J. Life Cycl.Assess. 6, 199–210.
Krewski, D., Jerrett, M., Burnett, R.T., Ma, R., Hughes, E., Shi, Y., Turner, M.C., Pope III, C.A., Thurston III, G., Calle III, E.E., Thun III, M.J., 2009. Extended Follow-up and Spatial Analysis of the American Cancer Society Study Linking Particulate Air Pollution and Mortality; Research Report 140, Health Effects Institute, Boston, MA. May (assessed 29 April, 2019) https://www.healtheffects.org/system/files/Krewski140.pdf.
Lepeule, J., Laden, F., Dockery, D., Schwartz, J., 2012. Chronic exposure to fine particles and mortality: an extended follow-up of the Harvard six cities study from 1974 to 2009. Environ. Health Persp. 120, 965–970.
Levy, J.I., Wilson, A.M., Zwack, L.M., 2007. Quantifying the efficiency and equity implications of power plant air pollution control strategies in the United States. Environ. Health Perspect. 115 (5), 743–750.
Levy, J.I., Baxter, L.K., Schwartz, J., 2009. Uncertainty and variability in health-related damages from coal-fired power plants in the United States. Risk Anal. 29, 1000–1014.
Logue, J.M., Small, M.J., Robinson, A.L., 2011. Evaluating the National Air Toxics Assessment (NATA): comparison of predicted and measured air toxics concentrations, risks, and sources in Pittsburgh, Pennsylvania. Atmos. Environ 45, 476–484.
Millstein, D., Wiser, R., Bolinger, M., Barbose, G., 2017. The climate and air-quality benefits of wind and solar power in the United States. Nat. Energy 2, 17134.
Modeling Guidance for Demonstrating Air Quality Goals for Ozone, 2018. PM2.5, and Regional Haze; U.S. Environmental Protection Agency: Research Triangle Park, NC. https://www3.epa.gov/ttn/scram/guidance/guide/O3-PM-RH-Modeling_Guidance-2018.pdf.
NAAQS Table, 2018. U.S. Environmental Protection Agency: Washington, DC. (accessed 21 November 2018) https://www.epa.gov/criteria-air-pollutants/naaqs-table.
Notter, D.A., 2015. Life cycle impact assessment modeling for particulate matter: a new approach based on physico-chemical particle properties. Environ. Int. 82, 10–20.
Ögmundarson, Ó., Sukumara, S., Laurent, A., Fantke, P., 2020. Environmental hotspots of lactic acid production systems. GCB Bioenergy 12, 19–38.
Particle Source Apportionment Tool (PSAT)Wagstrom, K.M., Pandis, S.N., Yarwood, G., Wilson, G.M., Morris, R.E., 2008. Development and application of a computationally efficient particulate matter apportionment algorithm in a three-dimensional chemical transport model. Atmos. Environ. 42, 5650–5659.
Penn, S.L., Arunachalam, S., Woody, M., Heiger-Bernays, W., Tripodis, Y., Levy, J.I., 2017. Estimating state-specific contributions to PM2.5- and O3-related health burden from residential combustion and electricity generating unit emissions in the United States. Environ. Health Perspect. 125, 324–332.
Photochemical Air Quality Modeling, 2017. U.S. Environmental Protection Agency: Washington, DC. https://www.epa.gov/scram/photochemical-air-quality-modeling (accessed 20 March 2019).
Pope III, C.A., Cropper, M., Coggins, J., Cohen, A., 2015. Health benefits of air pollution abatement policy: role of the shape of the concentration–response function. J. Air Waste Manage. Assoc. 65, 516–522.
Pope III, C.A., Lefler, J.S., Ezzati, M., Higbee, J.D., Marshall, J.D., Kim, S.Y., Bechle, M., Gilliat, K.S., Vernon, S.E., Robinson, A.L., Burnett, R.T., 2019. Mortality risk and fine particulate air pollution in a large, representative cohort of U.SAdults. Environ. Health Perspect. 127, 077007.
Refinery Capacity Report, 2018. U.S. Energy Information Administration: Washington, DC. https://www.eia.gov/petroleum/refinerycapacity/ (accessed 28 April 2019).
Revision to the Guideline on Air Quality Models, 2015. Enhancements to the AERMOD Dispersion Modeling System and Incorporation of Approaches to Address Ozone and Fine Particulate Matter. Tech. rep., U.S. Environmental Protection Agency, Washington, DC. #2060-AS54 http://www.epa.gov/ttn/scram/11thmodconf/9930-11-OAR_AppendixW_Proposal.pdf (accessed 5 February 2018).
Rosenbaum, R.K., Huijbregts, M.A.J., Henderson, A.D., Margni, M., McKone, T.E., van de Meent, D., Hauschild, M.Z., Shaked, S., Li, D.S., Gold, L.S., Jolliet, O., 2011. USEtox human exposure and toxicity factors for comparative assessment of toxic emissions in life cycle analysis: sensitivity to key chemical properties. Int. J. Life Cycle Assess. 16, 710–727.
Schwartz, J.D., Wang, Y., Kloog, I., Yitshak-Sade, M., Dominici, F., Zanobetti, A., 2018. Estimating the effects of PM2.5 on life expectancy using causal modeling methods. Environ. Health Perspect. 126, 127002.
Scire, J.S., Strimaitis, D.G., Yamartino, R.J., 2000. A User's Guide for the CALPUFF Dispersion Model. Tech. Rep. Earth Tech, Inc., Concord, MA. http://www.src.com/calpuff/download/CALPUFF_UsersGuide.pdf (accessed 5 February 2018).
Sedlbauer, K., Braune, A., Humbert, S., Margni, M., Schuller, O., Fischer, M., 2007. Spatial differentiation in LCA—moving forward to more operational sustainability. Technikfolgenabsch€atzung—Theorie und Praxis 16, 24–31.
Seinfeld, J.H., Pandis, S.N., 2006. Atmospheric Chemistry and Physics: From Air Pollution to Climate Change. 2nd, ed. John Wiley & Sons, Inc., Hoboken, New Jersey.
Tang, L., Nagashima, T., Hasegawa, K., Ohara, T., Sudo, K., Itsubo, N., 2018. Development of human health damage factors for PM2.5 based on a global chemical transport model. Int. J. Life Cycl. Assess. 23, 2300–2310.
Technical Support Document for the Proposed PM NAAQS Rule, 2006. Response Surface Modeling, Tech. Rep. U.S. Environmental Protection Agency, Research Triangle Park, NC. http://www.epa.gov/scram001/reports/pmnaaqs_tsd_rsm_all_021606.pdf (accessed 22 November 2018).
Tessum, C.W., Marshall, J.D., Hill, J.D., 2012. A spatially and temporally explicit life cycle inventory of air pollutants from gasoline and ethanol in the United States. Environ. Sci. Techno.l 46, 11408–11417.
Tessum, C.W., Hill, J.D., Marshall, J.D., 2014. Life cycle air quality impacts of conventional and alternative light-duty transportation in the United States. Proc. Natl. Acad. Sci. U. S. A. 111, 18490–18495.
Tessum, C.W., Hill, J.D., Marshall, J.D., 2017. InMAP: a model for air pollution interventions. PLoS One 12, e0176131.
Thakrar, S.K., Goodkind, A.L., Tessum, C.W., Marshall, J.D., Hill, J.D., 2017. Life cycle air quality impacts on human health from potential switchgrass production in the United States. Biomass Bioenergy 114, 73–82.
The IPUMS National Historical Geographic Information System (NHGIS), 2018. University of Minnesota, Minneapolis, MN. https://data2.nhgis.org/main (accessed 18 August 2018).

U.S. Department of Energy, 2016. In: Langholtz, M.H., Stokes, B.J., Eaton, L.M. (Eds.), 2016 Billion-Ton Report: Advancing Domestic Resources for a Thriving Bioeconomy, Volume 1: Economic Availability of Feedstocks. Oak Ridge National Laboratory, Oak Ridge, TN . http://energy.gov/eere/bioenergy/2016-billion-ton-report.

U.S. EPA, 2019. Integrated Science Assessment (ISA) for Particulate Matter (Final Report, Dec 2019). U.S. Environmental Protection Agency, Washington, DC EPA/600/R-19/188.

User's Manual for the Co-Benefits Risk Assessment Health Impacts Screening and Mapping Tool (COBRA), 2012. Tech. rep. U.S. Environmental Protection Agency, Washington, DC. https://www.epa.gov/sites/production/files/2017-10/documents/cobra_user_manual_september2017_508_v2.pdf (accessed 5 February 2018).

Van Zelm, R., Huijbregts, M.A.J., Den Hollander, H.A., Van Jaarsveld, H.A., Sauter, F.J., Struijs, J., Van Wijnen, H.J., Van De Meent, D., 2008. European characterization factors for human health damage of PM10 and ozone in life cycle impact assessment. Atmos. Environ. 42, 441–453.

Van Zelm, R., Preiss, P., Van Goethem, T., Van Dingenen, R., Huijbregts, M., 2016. Regionalized life cycle impact assessment of air pollution on the global scale: damage to human health and vegetation. Atmos. Environ. 134, 129–137.

Vodonos, A., Awad, Y.A., Schwartz, J., 2018. The concentration-response between long-term PM2.5 exposure and mortality; a meta-regression approach. Environ. Res. 166, 677–689.

WRF-CHEM, 2018. National Center for Atmospheric Research, University Corporation for Atmospheric Research, Boulder, CO. https://www2.acom.ucar.edu/wrf-chem (accessed 20 February 2018).

Zhang, W., Capps, S.L., Hu, Y., Nenes, A., Napelenok, S.L., Russell, A.G., 2012. Development of the high- order decoupled direct method in three dimensions for particulate matter: enabling advanced sensitivity analysis in air quality models. Geosci. Model Dev. 5, 355–368.